Supplementary information

Modeling the binding and diffusion of receptor-targeted nanoparticles topically applied on fresh tissue specimens

Soyoung Kang[1†], Xiaochun Xu[2†], Eric Navarro[2], Yu Wang[1], Jonathan T.C. Liu[1,3], and Kenneth M. Tichauer[2*]

[1] Department of Mechanical Engineering, University of Washington, Seattle, WA 98105

[2] Department of Biomedical Engineering, Illinois Institute of Technology, Chicago, IL 60616

[3] Department of Pathology, University of Washington School of Medicine, Seattle, WA 98105

[†] These authors contributed equally to this work

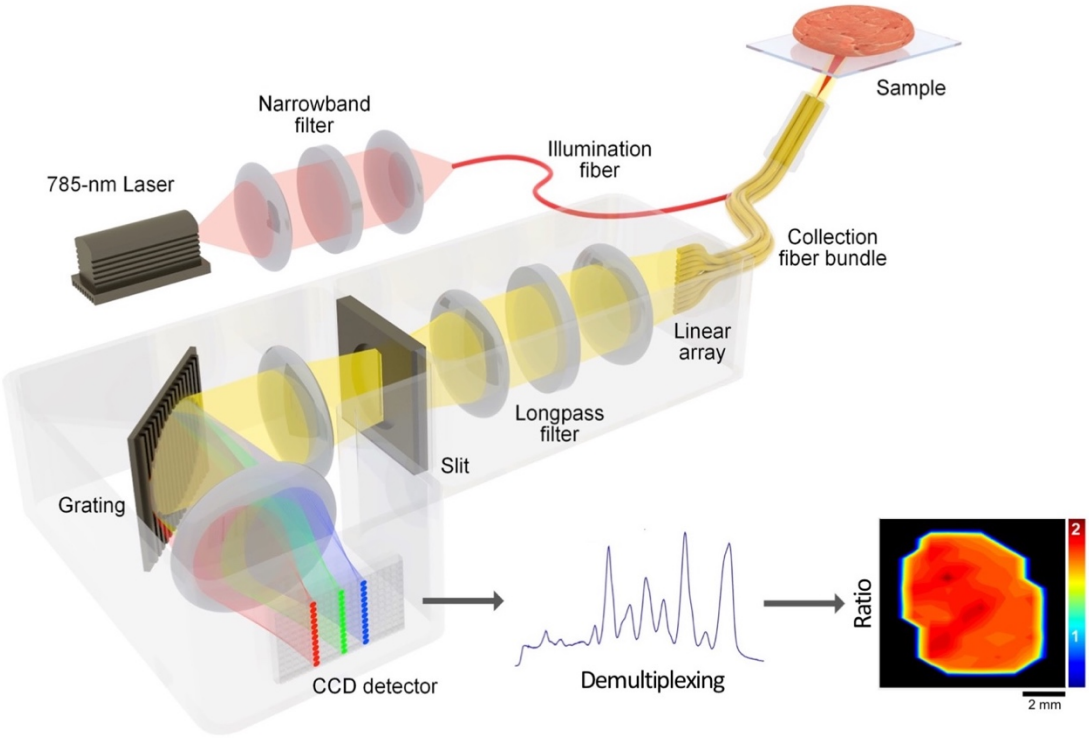

***Supplementary Figure 1. Raman-encoded molecular imaging (REMI) for* ratiometric wide-area imaging of fresh tissue topically stained with NPs.** A 10-mW 785-nm diode laser illuminates tissue with a spot size of ~1 mm. A custom spectrometer disperses the collected signal onto a cooled deep-depletion spectroscopic CCD. Raster-scanned spectral imaging of the sample is performed by scanning the tissue sample while keeping the fiber-bundle imaging probe stationary. A direct classical least-squares (DCLS) demultiplexing method is used to compute the relative NP weights and the weights of all broadband background components. The ratio of the weights of targeted to control NPs is used to obtain a ratiometric image of the tissue specimen. This imaging device has been described previously [1–5].

Sensitivity Analysis

A previously described multi-parametric sensitivity analysis (MPSA) method [6–11] was implemented to quantify the relative sensitivity of the model to various model parameters. MPSA classifies the influence that various parameters have on the model output of a simulation (in this case, the depth-integrated NP ratio) into two classes (*e.g.*, higher or lower output than the average output). Samples are then sorted according to each parameter independently, and cumulative distributions of the samples within the two classes are computed. The largest difference between these distributions (called the Kolmogorov-Smirnov, K-S, distance) serves as a metric indicating how strong the simulation output correlates to that specific parameter (*i.e.*, how sensitive the quantity that the filter is based on the uncertainty in that specific parameter). A larger K-S score indicates that the model is

more sensitive to variations in that parameter. The uncertainty of each parameter is determined in the analysis by randomly selecting parameter values from within a defined probability distribution (parameter range). A Monte Carlo strategy is then used in which the model is run repeatedly across the probability distributions of all the parameters. Here, it is initially assumed that all parameters have a very large inaccuracy (*i.e.*, six orders of magnitude that cover all feasible parameter values). **Supplementary Fig. 2** shows the sensitivity-based MPSA of our model parameters (k_3, k_4, k_5, k_6, D, and v_f), as well as staining concentration (C_0), staining time (t_{st}), and rinse time(t_r). Here, MPSA was run for a sample size of 100 Monte Carlo samples.

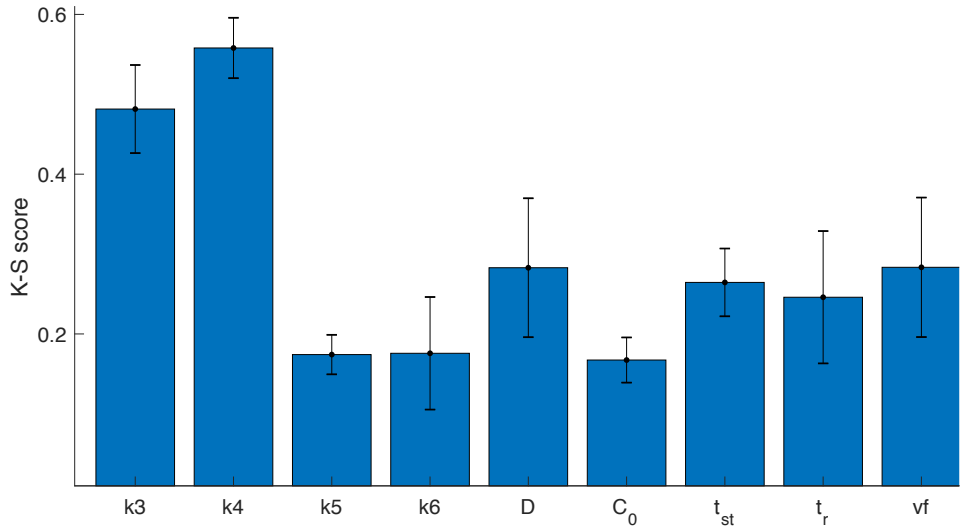

Supplementary Figure 2. The multi-parametric sensitivity analysis (MPSA) of various model parameters including: rate constants describing the targeted NP association and dissociation to its target receptor, k_3 and k_4, respectively; nonspecific association and dissociation of both targeted and control NPs, k_5 and k_6, respectively; diffusion rate constant, D; NP staining concentration, C_0; staining and rinse time, t_{st} and t_r, respectively; and volume fraction, v_f. The bars represent the sensitivity (K-S score) for each parameter. The MPSA sample size was 100 Monte Carlo samples and the error bars represent N=5 multi-parametric sensitivity analysis simulations.

Finite difference approximation to the model (Crank-Nicholson)

The numerical solution to the system of differential equations governing targeted NP diffusion and binding when topically applied to thick tissues requires discretization of the dependent variables (C_f, the concentration of unbound, "free" NPs; C_b, the concentration of NPs bound specifically; C_{ns}, the concentration of NPs bound nonspecifically to the tissue surface) into increments of depth, Δz, and time, Δt:

$$\begin{aligned} u_{k,n} &= C_f\left(\left(k-1\right)\Delta z,\left(n-1\right)\Delta t\right) \\ v_{k,n} &= C_b\left(\left(k-1\right)\Delta z,\left(n-1\right)\Delta t\right) \\ w_n &= C_{ns}\left(\left(n-1\right)\Delta t\right), \end{aligned} \tag{S1}$$

where $k = 1{:}N_z$ (N_z is the number of depth elements) is the k^{th} interval of depth, and $n = 1{:}N_t$ (N_t is the number of time elements) is the n^{th} interval of time. The parabolic partial differential equation set, **Eqs. (S1)**, for the targeted NP can be represented in finite differences using a Crank-Nicholson method as:

$$\begin{aligned} -\frac{D}{2\Delta z^2}u_{k-1,n+1} + \left(\frac{1}{\Delta t} + \frac{D}{\Delta z^2} + \frac{k_3}{2}\right)u_{k,n+1} - \frac{D}{2\Delta z^2}u_{k+1,n+1} - \frac{k_4}{2}v_{k,n+1} &= \frac{D}{2\Delta z^2}u_{k-1,n} + \dots \\ \dots + \left(\frac{1}{\Delta t} - \frac{D}{\Delta z^2} - \frac{k_3}{2}\right)u_{k,n} + \frac{D}{2\Delta z^2}u_{k+1,n} + \frac{k_4}{2}v_{k,n} & \\ -\frac{k_3}{2}u_{k,n+1} + \left(\frac{1}{\Delta t} + \frac{k_4}{2}\right)v_{k,n+1} &= \frac{k_3}{2}u_{k,n} + \left(\frac{1}{\Delta t} - \frac{k_4}{2}\right)v_{k,n}. \end{aligned} \tag{S2}$$

The initial condition was represented as:

$$u_{k,1} = 0,\ k \neq 1$$
$$u_{1,1} = v_f C_S\left(0\right) \tag{S3}$$

The control NP equations can be obtained by setting $k_3 = 0$.

Boundary conditions for the model

The numerical solution of the boundary conditions for the dependent variables, "free" and "nonspecific" retention of NPs, at the tissue surface were set to be:

$$u_{1,n} = v_f C_S\left(\left(n-1\right)\Delta t\right)$$
$$-\frac{k_5}{2}u_{1,n+1} + \left(\frac{1}{\Delta t} + \frac{k_6}{2}\right)w_{n+1} = \frac{k_5}{2}u_{1,n} + \left(\frac{1}{\Delta t} - \frac{k_6}{2}\right)w_n. \tag{S4}$$

The boundary condition of "free" NPs at the tissue edge distal to the staining surface, defined by the spatial derivative of the free NP concentration equal to zero, was expressed numerically as:

$$\frac{\nabla u_{N_z,t}}{\Delta z} = 0, \tag{S5}$$

which can be represented in backward finite differences of order Δz^2 as:

$$\nabla u_{k,n} = \frac{3}{2}u_{k,n} - 2u_{k-1,n} + \frac{1}{2}u_{k-2,n}. \tag{S6}$$

Solving the finite difference approximations to the model

Equations (S1)-(S6) were used to estimate $(n+1)^{\text{th}}$ diffusion and binding profiles, p_{n+1}, from the n^{th} diffusion and binding profile, p_n, by solving the following linear system:

$$\mathbf{X}p_{n+1} = \mathbf{Y}p_n, \tag{S7}$$

with the mldivide() function in MATLAB, where the matrices **X** and **Y** can be represented as:

$$\mathrm{X} = \begin{bmatrix}
1 & 0 & \cdots & \cdots & \cdots & 0 & 0 & \cdots & \cdots & \cdots & \cdots & 0 & 0 \\
-\frac{D}{2\Delta z^2} & \frac{1}{\Delta t}+\frac{D}{\Delta z^2}+\frac{k_3}{2} & -\frac{D}{2\Delta z^2} & & & \vdots & \vdots & -\frac{k_4}{2} & & & & \vdots & \vdots \\
0 & \ddots & \ddots & \ddots & & \vdots & \vdots & & \ddots & & & \vdots & \vdots \\
\vdots & & \ddots & \ddots & \ddots & 0 & \vdots & & & \ddots & & \vdots & \vdots \\
\vdots & & & -\frac{D}{2\Delta z^2} & \frac{1}{\Delta t}+\frac{D}{\Delta z^2}+\frac{k_3}{2} & -\frac{D}{2\Delta z^2} & \vdots & & & & -\frac{k_4}{2} & \vdots & \vdots \\
0 & \cdots & 0 & \frac{1}{2} & -2 & \frac{3}{2} & 0 & \cdots & \cdots & \cdots & \cdots & 0 & 0 \\
-\frac{k_3}{2} & 0 & \cdots & \cdots & \cdots & 0 & \frac{1}{\Delta t}+\frac{k_4}{2} & 0 & \cdots & \cdots & \cdots & 0 & 0 \\
0 & \ddots & & & & \vdots & 0 & \ddots & & & & \vdots & \vdots \\
\vdots & & \ddots & & & \vdots & \vdots & & \ddots & & & \vdots & \vdots \\
\vdots & & & \ddots & & \vdots & \vdots & & & \ddots & & \vdots & \vdots \\
\vdots & & & & \ddots & 0 & \vdots & & & & \ddots & 0 & \vdots \\
0 & \cdots & \cdots & \cdots & 0 & -\frac{k_3}{2} & 0 & \cdots & \cdots & \cdots & 0 & \frac{1}{\Delta t}+\frac{k_4}{2} & 0 \\
-\frac{k_5}{2} & 0 & \cdots & \cdots & \cdots & \cdots & \cdots & \cdots & \cdots & \cdots & \cdots & 0 & \frac{1}{\Delta t}+\frac{k_6}{2}
\end{bmatrix}, \tag{S8}$$

$$
Y = \begin{bmatrix}
1 & 0 & \cdots & \cdots & \cdots & 0 & 0 & \cdots & \cdots & \cdots & \cdots & 0 & 0 \\
\frac{D}{2\Delta z^2} & \frac{1}{\Delta t}-\frac{D}{\Delta z^2}-\frac{k_3}{2} & \frac{D}{2\Delta z^2} & & & \vdots & \vdots & \frac{k_4}{2} & & & & \vdots & \vdots \\
0 & \ddots & \ddots & \ddots & & \vdots & \vdots & & \ddots & & & \vdots & \vdots \\
\vdots & & \ddots & \ddots & \ddots & 0 & \vdots & & & \ddots & & \vdots & \vdots \\
\vdots & & & \frac{D}{2\Delta z^2} & \frac{1}{\Delta t}-\frac{D}{\Delta z^2}-\frac{k_3}{2} & \frac{D}{2\Delta z^2} & \vdots & & & & \frac{k_4}{2} & \vdots & \vdots \\
0 & \cdots & 0 & \frac{1}{2} & -2 & \frac{3}{2} & 0 & \cdots & \cdots & \cdots & \cdots & 0 & 0 \\
\frac{k_3}{2} & 0 & \cdots & \cdots & \cdots & 0 & \frac{1}{\Delta t}-\frac{k_4}{2} & 0 & \cdots & \cdots & \cdots & 0 & 0 \\
0 & \ddots & & & & \vdots & 0 & \ddots & & & & \vdots & \vdots \\
\vdots & & \ddots & & & \vdots & \vdots & & \ddots & & & \vdots & \vdots \\
\vdots & & & \ddots & & \vdots & \vdots & & & \ddots & & \vdots & \vdots \\
\vdots & & & & \ddots & 0 & \vdots & & & & \ddots & 0 & \vdots \\
0 & \cdots & \cdots & \cdots & 0 & \frac{k_3}{2} & 0 & \cdots & \cdots & \cdots & 0 & \frac{1}{\Delta t}-\frac{k_4}{2} & 0 \\
\frac{k_5}{2} & 0 & \cdots & \cdots & \cdots & \cdots & \cdots & \cdots & \cdots & \cdots & \cdots & 0 & \frac{1}{\Delta t}-\frac{k_6}{2}
\end{bmatrix}, \qquad \text{(S9)}
$$

where all the blank space in the matrix were 0s. p_n combines the free, bound and nonspecific retention compartments at all layers as:

$$
p_n = \begin{bmatrix}
u_{1,n} \\
u_{2,n} \\
u_{3,n} \\
\vdots \\
u_{N_z,n} \\
v_{1,n} \\
v_{2,n} \\
v_{2,n} \\
\vdots \\
v_{N_z,n} \\
w_n
\end{bmatrix}. \qquad \text{(S10)}
$$

The Matlab function mldivide was used to solve the vector p_{n+1} in the system of linear equations.

References

1. Wang Y, Kang S, Doerksen JD, Glaser AK, Liu JTC. Surgical guidance via multiplexed molecular imaging of fresh tissues labeed with SERS-coded nanoparticles. IEEE J Quantum Electron. 2016;22. Available: http://ieeexplore.ieee.org/xpls/abs_all.jsp?arnumber=7350220

2. Wang YW, Khan A, Som M, Wang D, Chen Y, Leigh SY, et al. Rapid ratiometric biomarker detection with topically applied SERS nanoparticles. Technology. 2014;2: 118–132. doi:10.1142/S2339547814500125

3. Wang YW, Reder NP, Kang S, Glaser AK, Yang Q, Wall MA, et al. Raman - encoded molecular imaging (REMI) with topically applied SERS nanoparticles for intraoperative guidance of lumpectomy. Cancer Res. 2017; doi:10.1158/0008-5472.CAN-17-0709

4. Wang YW, Doerksen JD, Kang S, Walsh D, Yang Q, Hong D, et al. Multiplexed Molecular Imaging of Fresh Tissue Surfaces Enabled by Convection-Enhanced Topical Staining with SERS-Coded Nanoparticles. Small. 2016;12: 5612–5621. doi:10.1002/smll.201601829

5. Kang S, Wang Y, Reder NP, Liu JTC. Multiplexed molecular imaging of biomarker-targeted SERS nanoparticles on fresh tissue specimens with channel-compressed spectrometry. PLoS One. 2016;11: 1–13. doi:10.1371/journal.pone.0163473

6. Spear RC, Hornberger GM. Eutrophication in Peel Inlet-II. Identification of Critical Uncertainties Via Generalized Sensitivity Analysis. Water Res. 1980;14: 43–49.

7. Cho KH, Shin SY, Kolch W, Wolkenhauer O. Experimental Design in Systems Biology, Based on Parameter Sensitivity Analysis Using a Monte Carlo Method: A Case Study for the TNF -Mediated NF- B Signal Transduction Pathway. Simulation. 2003;79: 726–739. doi:10.1177/0037549703040943

8. Zi Z, Cho KH, Sung MH, Xia X, Zheng J, Sun Z. In silico identification of the key components and steps in IFN-γ induced JAK-STAT signaling pathway. FEBS Lett. 2005;579: 1101–1108. doi:10.1016/j.febslet.2005.01.009

9. Tiemann CA, Vanlier J, Oosterveer MH, Groen AK, Hilbers PAJ, van Riel NAW. Parameter Trajectory Analysis to Identify Treatment Effects of Pharmacological Interventions. PLoS Comput Biol. 2013;9. doi:10.1371/journal.pcbi.1003166

10. Jeneson J a L, Schmitz JPJ, van den Broek NM a, van Riel N a W, Hilbers P a J, Nicolay K, et al. Magnitude and control of mitochondrial sensitivity to ADP. Am J Physiol Endocrinol Metab. 2009;297: E774–E784. doi:10.1152/ajpendo.00370.2009

11. Yoon J, Deisboeck TS. Investigating differential dynamics of the MAPK signaling cascade using a multi-parametric global sensitivity analysis. PLoS One. 2009;4. doi:10.1371/journal.pone.0004560